WAVELET FILTER EVALUATION FOR IMAGE WATERMARKING

Shih-Hsuan Yang

Department of Computer Science and Information Engineering
National Taipei University of Technology

ABSTRACT

Efficient image watermarking techniques have been developed in the wavelet domain. Similar to other wavelet-based image processing, the choice of wavelet filters generally affects the performance of a wavelet-based watermarking system. In this paper, we evaluate the performance of a set of biorthogonal integer wavelets under a multiresolution-watermarking framework. Biorthogonal integer wavelets have been extensively used for image applications because they possess the linear-phase property and can be efficiently implemented. We find that the widely adopted 9/7-F wavelet achieves the best robustness performance. Further investigation is conducted to show that the superiority of the 9/7-F wavelet is primarily owing to its being nearly orthogonal.

1. INTRODUCTION

In the last decade digital multimedia data have proliferated with the rapid developments of PC and Internet. The digital technology provides many advantages, including error-free reproduction, efficient processing and storage, and a uniform format for multimedia applications. These advantages, however, may hinder content owners from offering digital services because their revenues may be jeopardized due to perfect and rapid dissemination of unprotected digital contents. A watermark is an imperceptible code that remains present and detectable even if the media is processed and consumed by end users, and therefore can be used as a proof of copyright ownership.

To be valid for copyright protection, an image watermarking system should meet the following requirements [1]:

- Transparency. The embedded watermark should degrade the perceptual quality of host media to a minimal degree.
- Robustness. Any attack that erases the embedded watermark should render the host image useless.
- Adequate complexity. This issue is critical especially for real-time applications.

Image watermarking can be performed either in the spatial domain or in the transform domain. Spatial-domain techniques directly modulate the pixels while transform-domain techniques modify the DCT [2] (discrete cosine transform) or DWT [3] (discrete wavelet transform) coefficients. Transform-domain techniques usually achieve better performance since the perceptual characteristics of images can be better utilized and the spread spectrum principles used in secure communications can be easily incorporated. Multiresolution analysis with wavelet transforms has become the major vehicle for efficient image coding algorithms including the new JPEG-2000 standard [4]. The eligible basis functions for multiresolution analysis, however, are not unique. A natural and important question thus arises: "What is the best basis (wavelet) for use?" This question is almost answered for image compression. Both theoretical derivations and experimental evaluations have been extensively conducted [5]-[7]. The 'best' wavelets (9/7 and 5/3) have been chosen for the JPEG-2000 standard. The same issue, however, has not been resolved for image watermarking. This paper tries to answer the 'best-basis' problem for multiresolution image watermarking systems using biorthogonal wavelets.

In the following, we first review some fundamental knowledge about biorthogonal wavelet transforms. We then describe our wavelet evaluation platform for image watermarking. Simulation results along with analyses are presented next, followed by the conclusion.

2. BIORTHOGONAL INTEGER WAVELET TRANSFORMS

Favorable properties of wavelets include [8]:

- Desirable time-frequency localization.
- Compact support.
- Orthogonality.
- Smoothness, regularity, or vanishing moments.
- Symmetry (linear-phase constraint).

The above requirements may be conflicting. For example, the only real-valued orthogonal linear-phase wavelet with compact support is the trivial Haar filter. By relaxing the orthogonality constraint, most image applications employ the linear-phase biorthogonal FIR wavelets. This subclass of wavelets permits perfect reconstruction by symmetric extension across boundaries, avoiding the coefficient expansion and border discontinuity introduced by using circular convolution together with periodic extension. Additionally, the linear-phase biorthogonal wavelets can be efficiently implemented in the lifting framework [9], [10].

In this paper, we consider the biorthogonal integer wavelet transforms (IWT) under the lifting structure for performance evaluation. The seven IWT under study are the 5/3, 5/11-A, 5/11-C, 9/7-M, 9/7-F, 13/7-C, and 13/7-T, all tabulated in reference [7]. IWT is a fixed-point approximation to its parent linear transform, and can be implemented without resorting to costly floating-point operations. It is reversible and suitable for a unified lossy and lossless codec. Furthermore, the degradation introduced by the integer approximation is often very small [7], [11].

When applied to coding and watermarking, the wavelet transforms may require proper normalization. For a dyadic multiresolution system, the scaling function coefficients (i.e., the lowpass filter) $\{h(n)\}$ should be normalized for convergence as [8]

$$\sum_n h(n) = \sqrt{2} \qquad (1)$$

Some properties of the seven wavelets are given in Table 1.

Table 1: Some properties of the wavelets under study. The vanishing moments *M*/*N* are for the analyzing and synthesizing filters, respectively [7]. NOM will be addressed in Section 4.

	5/3	5/11-A	5/11-C	9/7-M	9/7-F	13/7-C	13/7-T
Vanishing moments	2/2	2/2	4/2	4/2	4/4	4/2	4/4
Coding gain	6.277	6.300	6.280	6.181	5.916	6.260	6.241
NOM	1.438	1.438	1.438	1.347	1.040	1.310	1.300

3. EVALUATION PLATFORM

We follow the multiresolution-watermarking framework reported in [3] as our wavelet filter evaluation platform. A p-level two-dimensional pyramidal DWT in one of the seven types is performed to generate $(3p + 1)$ subbands. We index these subbands from 0 to $3p$ in a parent-to-child order. Subband 0 is an approximation to the original image while the other subbands provide details. According to the spread-spectrum principle, a watermark signal $\mathbf{w} = \{w_i, i = 1, 2,\ldots, n\}$ of length n is cast upon n selected wavelet coefficients over various subbands. The locations of these watermark-bearing coefficients **p** should be recorded along with the original wavelet coefficients **x** and the watermark signal **w**, to be the private keys for watermark extraction. Taking the self-masking effects into consideration, a multiplicative watermarking scheme is adopted. A wavelet coefficient x_k is modified by w_k to y_k as

$$y_k = x_k(1 + \alpha w_k) \tag{2}$$

where the strength factor α determines the watermarking energy that balances transparency and robustness.

For watermark identification, the image under dispute of copyright violation performs the same multiresolution analysis as in the watermark-embedding process. The obtained wavelet coefficient y_k^* would be a distorted version of y_k due to intentional attacks or unintentional image processing. The watermark sequence **w*** is retrieved from y_k^* by

$$w_k^* = \frac{y_k^* - x_k}{\alpha x_k} \tag{3}$$

with the aid of private keys **p** and **x**. The similarity of the extracted pattern **w*** and the original watermark signal **w** can be measured by the correlation coefficient

$$\rho(\mathbf{w}, \mathbf{w}^*) = \frac{<\mathbf{w}, \mathbf{w}^*>}{\|\mathbf{w}\|_2 \|\mathbf{w}^*\|_2} \tag{4}$$

where <., .> denotes the inner product and $\|.\|_2$ denotes the 2 norm. A value of ρ that is close to 1 indicates a high degree of similarity. An appropriate threshold on ρ for copyright confirmation is determined to compromise the probabilities of false positive and false negative.

Common parameters of the described multiresolution watermarking system for our simulation are summarized below:

- Number of levels of DWT (p): 5.
- Test images: 512 × 512, 8 bpp (bits per pixel) gray-scale images Lena and Baboon.
- The watermark signal **w** is collected from an independent identically distributed Gaussian random source of zero mean and unit variance.
- The strength factor α is adjusted to allow the maximal robustness without noticeable degradation. We make the watermarked images with different wavelet transforms have the same peak signal-to-noise ratio (PSNR) for a fair comparison. The watermarked Lena and Baboon have PSNR equal to 35.6 dB and 38.4 dB, respectively, as shown in Fig. 1.
- The proposed system is evaluated against a set of default noise-like attacks included in the StirMark benchmark system [12]. The examined attacks are sharpening, Gaussian filtering, FMLR, 3×3 median filtering, and lossy JPEG compression with various quality factors.

(a)

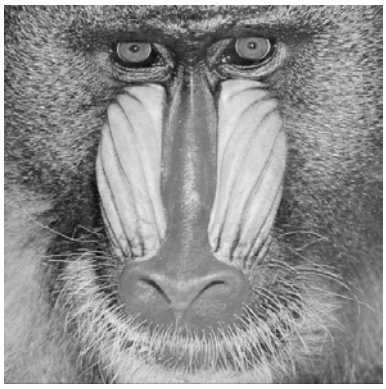

(b)

Fig. 1: The watermarked images using the 9/7-F wavelet, (a) Lena (PSNR= 35.6 dB), (b) Baboon (PSNR= 38.4 dB).

4. EXPERIMENTAL RESULTS AND ANALYSES

We consider two scenarios in sequence to investigate the robustness of the multiresolution watermarking system using different biorthogonal integer wavelets.

Scenario I:

- Subbands to embed: all subbands excluding the approximation layer (subband 0). It is observed that labeling the approximation layer results in visible artifacts. The largest n (in magnitude) wavelet coefficients are selected to embed the watermark.
- Length of the watermark signal (n): 1000.

The corresponding values of the strength factor α for different

wavelets are given in Table 2. The similarity results against attacks are given in Tables 3 and 4. We find the 9/7-F filter [5] provides consistently the best results, while the differences among the others are small. Since image compression shares many common characteristics with watermarking, in the following we discuss the wavelet-based image coding to shed some light on the wavelet-based watermarking.

Table 2: Strength factor α for watermarking in Scenario I.

	5/3	5/11-A	5/11-C	9/7-M	9/7-F	13/7-C	13/7-T
Lena	0.178	0.184	0.173	0.181	0.185	0.178	0.173
Baboon	0.190	0.181	0.177	0.192	0.181	0.190	0.189

Table 3: Scenario-I similarity tests for Lena.

	5/3	5/11-A	5/11-C	9/7-M	**9/7-F**	13/7-C	13/7-T
Sharpen-ing	0.363	0.347	0.321	0.261	**0.483**	0.293	0.294
Gaussian Filtering	0.688	0.695	0.676	0.651	**0.840**	0.638	0.622
FMLR	0.500	0.535	0.509	0.532	**0.604**	0.524	0.505
Median Filtering	0.314	0.296	0.286	0.278	**0.813**	0.212	0.251
JPEG 30	0.900	0.906	0.903	0.871	**0.970**	0.866	0.870
JPEG 20	0.841	0.844	0.834	0.776	**0.939**	0.781	0.758
JPEG 10	0.628	0.657	0.645	0.613	**0.832**	0.612	0.585

Table 4: Scenario-I similarity tests for Baboon.

	5/3	5/11-A	5/11-C	9/7-M	**9/7-F**	13/7-C	13/7-T
Sharpen-ing	0.178	0.164	0.115	0.193	**0.235**	0.169	0.164
Gaussian Filtering	0.376	0.365	0.379	0.313	**0.419**	0.340	0.332
FMLR	0.686	0.682	0.670	0.676	**0.730**	0.679	0.681
Median Filtering	0.544	0.506	0.507	0.500	**0.582**	0.525	0.482
JPEG 30	0.767	0.752	0.761	0.685	**0.890**	0.737	0.692
JPEG 20	0.637	0.600	0.628	0.566	**0.806**	0.613	0.571
JPEG 10	0.472	0.457	0.490	0.423	**0.655**	0.463	0.441

Modern wavelet image coders are derived from Shapiro's embedded zerotree wavelet (EZW) coding [13]. The EZW coding is an iterative algorithm, which not only efficiently removes the inter-scale redundancy across scales but also generates scalable bitstreams. Among the various improvements of EZW, the set partitioning in hierarchical trees (SPIHT) coding [14] is regarded as the simplest and most efficient. SPIHT has become a basis by which new image compression methods are compared. The SPIHT coding results for the seven filters are given in Tables 5 and 6. The arithmetic coding is not included in the coding algorithm since it provides only marginal improvement in rate reduction while involving intensive computation. We observe that the 9/7-F filter outperforms the others, as is for watermarking. The PSNR gap is significant, especially at low bit rates. Note that the low-rate results are particularly interesting to us since in the proposed scheme the watermark information is inserted in large wavelet coefficients that are found significant in early quantization iterations.

Table 5: SPIHT coding performance for Lena. The number indicates the PSNR (in dB) of the reconstructed image.

bpp	5/3	5/11-A	5/11-C	9/7-M	**9/7-F**	13/7-C	13/7-T
0.125	29.1	29.4	29.4	29.3	**30.3**	29.3	29.3
0.25	31.8	31.9	31.8	32.3	**33.2**	32.3	32.4
0.5	35.2	35.3	35.2	34.9	**36.1**	35.0	35.0
1.0	38.4	38.4	38.2	38.0	**38.3**	37.9	38.0

Table 6: SPIHT coding performance for Baboon. The number indicates the PSNR (in dB) of the reconstructed image.

bpp	5/3	5/11-A	5/11-C	9/7-M	**9/7-F**	13/7-C	13/7-T
0.125	20.2	20.0	19.8	20.5	**21.4**	20.6	20.5
0.25	22.1	22.1	22.0	21.8	**22.6**	22.0	21.9
0.5	24.5	24.5	24.4	24.3	**24.9**	24.4	24.4
1.0	27.6	27.6	27.5	27.3	**28.4**	27.4	27.4

Among the various attributes that may affect the performance of biorthogonal wavelets, we believe that the closeness to orthogonality may be dominant. Orthogonality implies energy preservation, and the sum of individual subband mean square errors (MSE) equals the overall MSE in the spatial domain. Consequently, efficient quantization and bit-allocation procedures can be directly developed in the transform domain for orthogonal wavelets. Typical coding (or watermarking) systems, however, employ the same quantization (or watermarking) procedures for both orthogonal and biorthogonal wavelets. Performance degradation is expected from the "energy mismatch" for biorthogonal wavelets. Several closeness measures on orthogonality for biorthogonal wavelets have been developed [15]-[17]. For example, the near-orthogonality measure (NOM) has been defined in [15] as

$$\mathrm{NOM} = \sum_n |h(n)|^2 \qquad (5)$$

NOM is the weighting factor of the lowpass subband distortion introduced by non-orthogonality. Orthogonal wavelets have the NOM value equal to 1 and the deviation of NOM from 1 can be regarded as the degree of non-orthogonality. The NOM values of the seven filters under study are listed in the last row of Table 1. It can be seen that the 9/7-F wavelet is 'almost' orthogonal; it is of no surprise since its parent linear wavelet is designed to approximate orthonormal filters [5].

Scenario II:

In contrast to compression where no subband can be discarded without distortion penalty, we can choose the watermarking subbands to be on the same level to avoid energy mismatch. The Scenario-II experiments proceed with the following modifications:

- Subbands to embed: only subbands 1 and 2. They are both on the lowest-frequency detail level.
- Length of the watermark signal (n): 256. That is, the largest (in magnitude) 256 coefficients out of the 512 coefficients within subbands 1 and 2 are modified.

The corresponding values of α for this scenario are given in Table 7. The similarity results are given in Tables 8 and 9. Two factors account for the general increase in correlation coefficients relative to Scenario I. First, the strength factor α increases with the smaller number of n. Second, the low-frequency subbands are more resilient to noise-like distortions. Note that the similarity gap

between 9/7-F and other wavelets becomes much less significant. This confirms our conjecture that orthogonality is the deciding factor for the robustness performance. For a multiresolution watermarking system using biorthogonal wavelets, a major challenge would therefore be to intelligently distribute the watermarking energy over the watermark-bearing wavelet coefficients. Besides, we have tested the linear (floating-point) versions of the employed filter banks and have concluded that the watermarking performance degradation introduced by integer approximation is small, as is for compression. Currently we are developing general watermarking schemes suitable for non-orthogonal wavelets.

Table 7: Strength factor α for watermarking in Scenario II.

	5/3	5/11-A	5/11-C	9/7-M	9/7-F	13/7-C	13/7-T
Lena	0.257	0.246	0.234	0.250	0.249	0.260	0.240
Baboon	0.288	0.282	0.270	0.280	0.294	0.272	0.288

Table 8: Scenario-II similarity tests for Lena.

	5/3	5/11-A	5/11-C	9/7-M	**9/7-F**	13/7-C	13/7-T
Sharpen-ing	0.827	0.745	0.692	0.756	**0.864**	0.843	0.768
Gaussian Filtering	0.950	0.943	0.918	0.935	**0.975**	0.950	0.933
FMLR	0.819	0.802	0.809	0.821	**0.897**	0.870	0.840
Median Filtering	0.702	0.984	0.659	0.710	**0.934**	0.724	0.680
JPEG 30	0.966	0.957	0.956	0.955	**0.978**	0.961	0.952
JPEG 20	0.943	0.938	0.931	0.925	**0.963**	0.947	0.936
JPEG 10	0.834	0.808	0.812	0.876	**0.878**	0.854	0.843

Table 9: Scenario-II similarity tests for Baboon.

	5/3	5/11-A	5/11-C	9/7-M	**9/7-F**	13/7-C	13/7-T
Sharpen-ing	0.648	0.600	0.608	0.664	**0.712**	0.607	0.652
Gaussian Filtering	0.938	0.939	0.900	0.906	**0.970**	0.921	0.912
FMLR	0.924	0.902	0.879	0.888	**0.955**	0.910	0.912
Median Filtering	0.836	0.856	0.887	0.848	**0.926**	0.837	0.846
JPEG 30	0.953	0.947	0.935	0.940	**0.973**	0.935	0.935
JPEG 20	0.935	0.931	0.919	0.900	**0.961**	0.929	0.914
JPEG 10	0.847	0.832	0.813	0.827	**0.897**	0.846	0.828

5. CONCLUSION

This paper tries to find the best biorthogonal wavelet filter for multiresolution image watermarking. Simulation is conducted under a spread-spectrum watermarking framework where a Gaussian distributed watermark is injected into the largest wavelet coefficients. We evaluate the robustness performance of seven integer biorthogonal wavelet bases. The 9/7-F wavelet provides a substantial edge when all detail subbands are eligible for watermarking. The performance gap shrinks when only subbands on the same level are watermarked, which substantiates the conjecture that the major merit of the 9/7-F wavelet for image watermarking is its orthogonality.

6. ACKNOWLEDGEMENT

This work is supported by the National Science Council, R. O. China, under the contract number NSC 90-2213-E-027-012.

REFERENCES

[1] I. J. Cox, M. L. Miller, and A. J. Bloom, *Digital Watermarking*, Morgan Kaufmann Publishers, 2002.

[2] I. J. Cox, J. Killian, F. T. Leighton, and T. Shamoon, "Secure spread spectrum watermarking for multimedia," *IEEE Trans. Image Process*., vol. 6, no. 12, pp. 1673-1687, Dec. 1997.

[3] W. Zhu, Z. Xiong, and Y.-Q. Zhang, "Multiresolution watermarking for images and video," *IEEE Trans. Circuits Syst. Video Technol*., vol. 9, no. 4, pp. 545-550, June 1999.

[4] B. Usevitch, "A tutorial on modern lossy wavelet image compression: foundations of JPEG 2000," *IEEE Signal Process. Mag*., vol. 18, no. 5, Sep. 2001.

[5] M. Antonini, M. Barlaud, P. Mathieu, and I. Daubechies, "Image coding using wavelet transform," *IEEE Trans. Image Processing*, vol. 1, no. 2, pp. 205-220, Apr. 1992.

[6] J. D. Villasenor, B. Belzer, and J. Liao, "Wavelet filter evaluation for image compression," *IEEE Trans. Image Processing*, vol. 4, no. 8, pp. 1053-1060, Aug. 1995.

[7] M. D. Adams and F. Kossentini, "Reversible integer-to-integer wavelet transforms for image compression: performance and analysis," *IEEE Trans. Image Processing*, vol. 9, no. 6, pp. 1010-1024, June 2000.

[8] C. S. Burrus, R. A. Gopinath, and H. Guo, *Introduction to Wavelets and Wavelet Transforms: A Primer*, Prentice-Hall, Inc., 1998.

[9] I. Daubechies and W. Sweldens, "Factoring wavelet transforms into lifting steps," *J. Fourier Anal. Appl.*, vol. 4, no. 3, pp. 247-269, 1998.

[10] A. R. Calderbank, I. Daubechies, W. Sweldens, and B.-L. Yeo, "Wavelet transforms that map integers to integers," *Appl. Comput. Harmon. Anal*., vol. 5 pp. 332-369, July 1998.

[11] J. Reichel, G. Menegas, M. J. Nadenau, and M. Kunt, "Integer wavelet transform for embedded lossy to lossless image compression," *IEEE Trans. Image Processing*, vol. 10, no. 3, pp. 383-392, Mar. 2001.

[12] StirMark version 3.1, http://www.cl.cam.ac.uk/~fapp2 /watermarking/stirmark/

[13] J. M. Shapiro, "Embedded image coding using zerotrees of wavelet coefficients," *IEEE Trans. Signal Processing*, vol. 41, no. 12, pp. 3445-3462, Dec. 1993.

[14] A. Said and W. A. Pearlman, "A new, fast, and efficient image codec based on set partitioning in hierarchical trees," *IEEE Trans. Circuits Syst. Video Technol.*, vol. 6, no. 3, pp. 243-250, June 1996.

[15] F. Moreau de Saint Martin, A. Cohen, and P. Siohan, "A measure of near-orthogonality of PR biorthogonal filter banks," *Proc. IEEE Int. Conf. Acoustics, Speech, Signal Processing*, Mar. 1995, pp. 1480-1483.

[16] F. Moreau de Saint Martin, P. Siohan, and A. Cohen, "Biorthogonal filterbanks and energy preservation property in image compression," *IEEE Trans. Image Process*., vol. 8, no. 2, pp. 168-178, Feb. 1999.

[17] B. Usevitch, "Optimal bit allocation for biorthogonal wavelet coding," *Proc. Data Compression Conf.*, Snowbird, UT, Mar. 1996, pp. 387-395.